

PAPER • OPEN ACCESS

# Commissioning of the Cryogenic Phase Equilibria Test Stand CryoPHAEQTS

To cite this article: J Tamson *et al* 2020 *IOP Conf. Ser.: Mater. Sci. Eng.* **755** 012150

View the [article online](#) for updates and enhancements.

# Commissioning of the Cryogenic Phase Equilibria Test Stand CryoPHAEQTS

J Tamson<sup>1</sup>, P Blanck<sup>1</sup>, S Grohmann<sup>1,2</sup>

<sup>1</sup>Karlsruhe Institute of Technology (KIT), Institute of Technical Thermodynamics and Refrigeration, Engler-Bunte-Ring 21, 76131 Karlsruhe, Germany

<sup>2</sup>Karlsruhe Institute of Technology (KIT), Institute of Technical Physics, Hermann-von-Helmholtz-Platz 1, 76344 Eggenstein-Leopoldshafen, Germany

E-mail: jens.tamson@kit.edu

**Abstract.** Medium-sized cryogenic applications such as local hydrogen liquefaction or HTS power applications require temperatures below 77 K at some kW cooling power. These conditions are efficiently reached by cryogenic mixed refrigerant cycles (CMRC). The CMRC development relies on physical property data of cryogenic fluid mixtures that is not available for most binary and multi-component systems. The cryogenic phase equilibria test stand CryoPHAEQTS provides precise physical property data of cryogenic fluid mixtures at temperatures from 15 K to 300 K and at pressures up to 150 bar. It also allows flammable mixtures (e.g. containing hydrogen) or oxidizing mixtures (e.g. containing oxygen). Vapor-liquid equilibria (VLE), vapor-liquid-liquid equilibria (VLLE) and the liquidus line of solid-liquid equilibria (SLE) are obtained by direct sampling from the equilibrium cell and analysis by gas chromatography. The equilibrium cell offers optical access by 4 windows to identify the coexisting phases. The cell temperature is set by a pulse-tube cryocooler and a counter-heater. As a unique feature, the specific heat capacity of the vapor phase in equilibrium is measured by the combination of a novel thermal and a Coriolis type flow meter. Having measured both caloric and thermal properties of the mixtures, we can develop new equations of state that cover all thermodynamic state variables. In this talk, we report on the progress in the construction and commissioning of CryoPHAEQTS. Validation of the measurement accuracy is presented by comparison of pure substances measurements against literature data.

## 1. Introduction

Process design calculations rely on precise physical property data of the working fluids. In particular, vapor-liquid equilibria (VLE) and vapor-liquid-liquid equilibria (VLLE) are crucial to the design of vapor compression cycles such as cryogenic mixed refrigerant cycles (CMRC). For pure working fluids, this physical property data is available through REFPROP[1]. At cryogenic temperatures, however, only a few binary mixtures have been investigated sufficiently. The cryogenic phase equilibria test stand CryoPHAEQTS at KIT allows phase equilibria measurements of all atoxic refrigerant mixtures. The test stand offers precise VLE and VLLE measurements in a temperature range from 15 K to 300 K and at pressures up to 150 bar. Before measuring unknown physical property data, the measurement accuracy of CryoPHAEQTS is validated against the nitrogen vapor pressure curve.

The test facility is briefly introduced in section 2, followed by the description of the measurement procedure in section 3. The results of the commissioning with pure nitrogen



are presented in section 4 and discussed in comparison to reference data. Final conclusions are drawn in section 5 together with an outlook on future work.

## 2. The CryoPHAEQTS test stand

A detailed description of the CryoPHAEQTS test stand is given in [2]. An isothermal analytical approach with sampling through capillaries and gas phase circulation is used, following the classification of Peper et al. [3].

The test stand includes an equilibrium cell installed in a high-vacuum cryostat. The cell has three sampling capillaries at different positions and an additional capillary for pressure measurement. The cell temperature is adjusted by the second stage of a pulse-tube cryocooler in combination with compensation heating. As shown in Figure 1, the temperature is measured with two temperature sensors in the wall of the equilibrium cell's main body. The upper sensor is closer to the vapor phase and the lower one closer to the liquid phase. On the horizontal axis, they are located at the same coordinate; on the vertical axis, they have the same distance to the center of the cell. The cell is surrounded by an aluminum radiation shield that is connected to the first stage of the cryocooler. Additionally, the compensation heater as well as most parts of the piping and the equilibrium cell are wrapped in multi-layer insulation.

The integral leak rate, measured in the vacuum cryostat with test gas in the fluid circuit at high and low temperatures and pressures up to 10 MPa, is lower than  $1 \times 10^{-9}$  mbar L<sup>-1</sup> s<sup>-1</sup>. Based on the lower temperature sensor in Figure 1, a low temperature limit of 15.799 K  $\pm$  8 mK is achieved. Due to yet insufficient thermal insulation of the cell, the upper temperature sensor shows an offset beyond the measurement uncertainty, yielding an average low temperature limit of 16.038 K  $\pm$  154 mK. At cryogenic temperatures, an insulating vacuum pressure of  $10^{-8}$  mbar is reached.

## 3. Measurement procedure

The fluid circuit is first evacuated and purged with nitrogen three times. For all measurements, nitrogen of type ALPHAGAZ 1 with a purity of 99.999 % supplied by Air Liquide is used. The

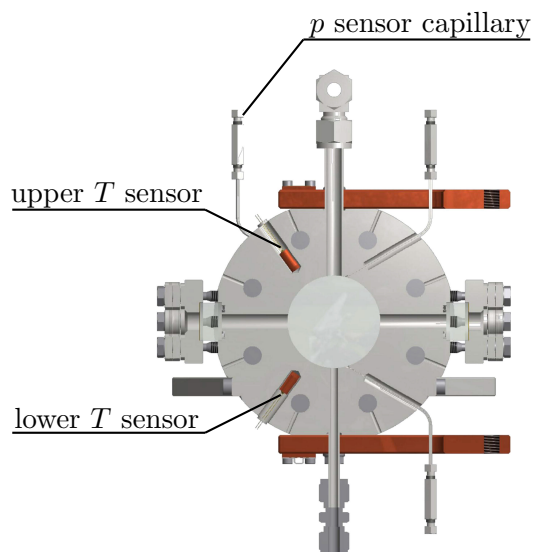


Figure 1: CAD model of the equilibrium cell with the pressure sensor capillary and two temperature sensors.

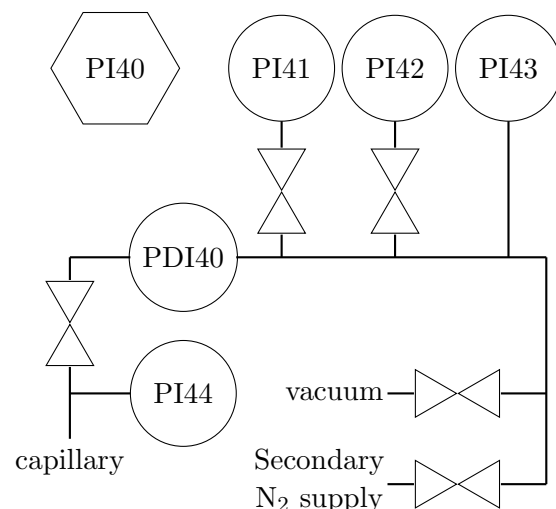


Figure 2: Secondary nitrogen system for precise pressure measurement.

Table 1: Sensors used in CryoPHAEQTS and their respective measurement ranges.

Tag	Type	Used measurement range
TI74/75	Cernox™ temperature sensors	15 K to 300 K
PI44	Absolute pressure sensor	0 bar(a) to 151 bar(a)
PI43	Relative pressure sensor	70 bar(g) to 150 bar(g)
PI42	Relative pressure sensor	10 bar(g) to 70 bar(g)
PI41	Relative pressure sensor	-1 bar(g) to 10 bar(g)
PI40	Absolute pressure sensor	750 mbar to 1150 mbar
PDI40	Differential pressure sensor	-50 mbar to 50 mbar

cryostat is evacuated simultaneously, reaching pressures of  $10^{-4}$  mbar. Afterwards, the nitrogen gas is circulated and cooled down continuously by the pulse-tube cryocooler. The equilibrium cell temperature is set by a temperature controller that electrically heats into the second stage of the cryocooler.

The measurement sequence starts as pressure and temperature in the equilibrium cell stabilize. Fluctuations of  $\pm 10$  mK per 10 min and  $\pm 10$  mbar per 10 min are accepted and considered steady-state, unless unidirectional. During the measurement sequence, the pressure of the secondary nitrogen system explained in [2] is adjusted to  $\pm 50$  mbar of the equilibrium cell pressure. Following Figure 2, the differential pressure sensor PDI40 determines the pressure difference between the secondary nitrogen system and the equilibrium cell. Dependent on the absolute pressure, the valves to the sensors PI41 or PI42 are opened according to their respective measurement ranges shown in Table 1. All pressure sensors and valves are located in proximity to the cryostat at ambient conditions. The sensors PI44 and PDI40 are connected to the measurement cell through a 2 m long capillary and a vacuum feedthrough. With a sampling rate of 200 mHz, temperature and pressure data is recorded for 10 min.

#### 4. Results and discussion

Phase equilibrium data for nitrogen are measured in a range from 65.433 K to 125.838 K, corresponding to a pressure range of 0.191 bar to 33.612 bar. The results are listed in Table 2 and plotted in Figures 3 and 4. Measurement uncertainties are calculated according to GUM [4]. Applying a confidence interval of 95 % (i.e.  $k = 2 = 2\sigma$ ), the uncertainty in temperature measurement ranges from  $\pm 7$  mK to  $\pm 34$  mK for each sensor, and from  $\pm 54$  mK to  $\pm 119$  mK for the mean temperature. The uncertainty in pressure measurement ranges from  $\pm 0.3$  mbar to  $\pm 3.6$  mbar.

Figure 3 shows the vapor-liquid coexistence curve of nitrogen taken from the REFPROP 10.0 equation of state (REFPROP EOS) and the experimental data of this work. Figure 4 presents the relative pressure deviations with regard to the REFPROP EOS, adding up to an average absolute deviation (AAD) of 0.8 %. The relative error bars of the pressure measurement become smaller with increasing temperature, since the absolute uncertainty shown in table 2 is in the mbar range, while the pressure increases from 0.191 bar to 33.612 bar.

Over the entire range, there is a temperature offset between the lower and the upper sensor of up to 220 mK, indicating temperature stratification in the equilibrium cell. At higher temperatures, the measured vapor pressures are about 0.7 % lower than the values obtained from the REFPROP EOS. This may indicate a systematic error in the temperature measurement, yielding lower temperatures than the actual fluid temperature. Such systematic error can origin from thermal radiation, thermal conduction and convection.

Table 2: Experimental vapor-liquid equilibrium data for nitrogen containing the mean temperature  $T$ , pressure  $p$ , uncertainties  $u$  and relative deviations  $p-p_{\text{ref}}/p_{\text{ref}}$  between the experimental data and the REFPROP database.

Temperature $T$ in K	Pressure $p$ in bar	Uncertainty $u(T)$ in mK	Uncertainty $u(p)$ in mbar	Deviation to [1] in %
65.433	0.1910	75	0.3	-1.9
73.804	0.6447	72	1.1	-1.2
81.467	1.6028	64	1.5	0.0
88.165	3.0865	54	2.8	0.5
95.092	5.4865	74	0.6	0.8
102.728	9.4428	55	0.7	0.7
110.994	15.6404	65	3.0	0.6
119.365	24.4787	75	3.6	0.7
125.838	33.6115	87	3.5	0.7

The equilibrium cell has two large glass windows exposed to thermal radiation from the inner cryostat wall at ambient temperature. At about 80 K, the negative deviations with regard to the REFPROP EOS change to positive values. At the same temperature, the equilibrium cell temperature starts to be lower than the radiation shield temperature, changing the direction of the net radiation heat transfer. Above 80 K, the cell is cooled by radiation to the cooler shield surface, whereas below 80 K, the cell is exposed to an additional radiation heat from the warmer shield. By enhanced radiation shielding using multi-layer insulation, the thermal radiation on/from the cell shall be further reduced, yielding smaller temperature gradients and a lower minimum temperature. A shield temperature management that, within the boundaries of the cryocooler performance, keeps the shield temperature close the cell temperature, may further improve the cell temperature homogeneity.

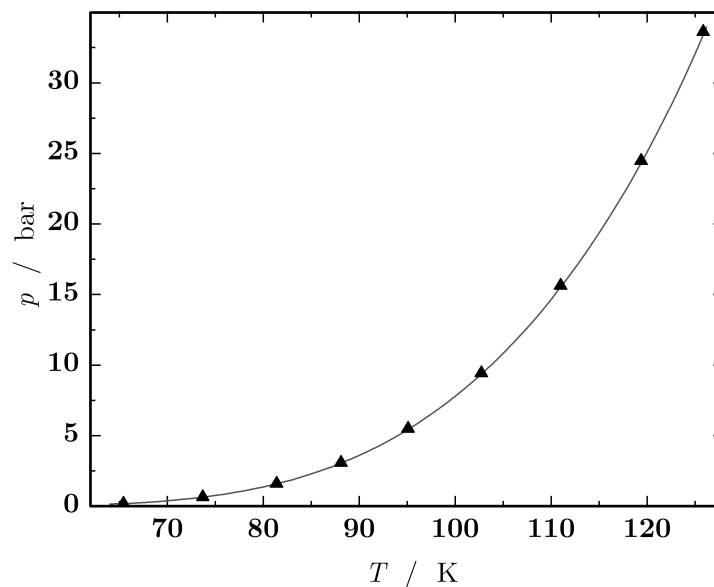


Figure 3: Vapor-liquid coexistence curve of nitrogen. The continuous line represents data from Span et al. [5] and the triangles mark the data from this work.

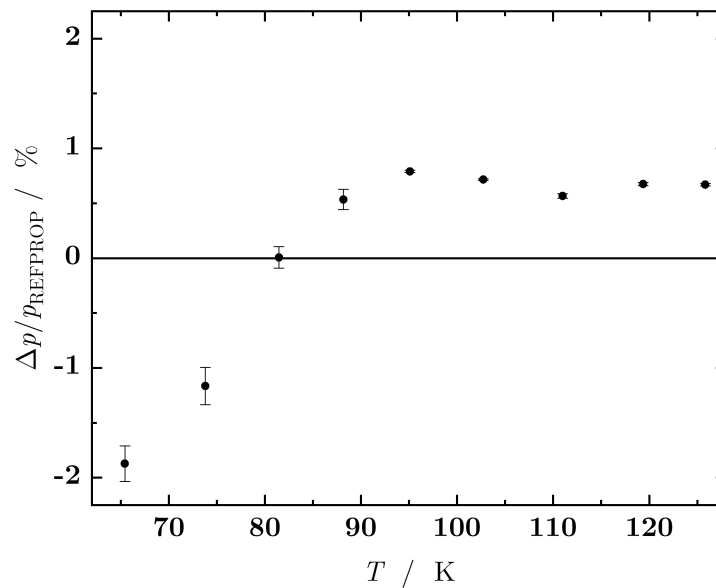


Figure 4: Relative pressure deviations  $p-p_{\text{ref}}/p_{\text{ref}}$  of the data from this work from the REFPROP EOS, including relative pressure measurement uncertainties.

In addition, the two conductive heat links between the equilibrium cell and the cryocooler, one attached on top and one at the bottom of the cell, may perform slightly different despite equivalent thermal conduction lengths. Contact improvements may yield a more homogenous temperature field in the equilibrium cell wall.

To study heat convection phenomena in the cell, the temperature offset is recorded with and without gas phase circulation. At around 95 K, the temperature offset increased by 110 mK when turning off the circulation. At this temperature, the thermal conductivity of the saturated liquid phase is about 10 times higher than in the saturated vapor. Compared to the liquid phase, the vapor phase is more likely to have internal gradients between the boundary layer at the wall and the bulk. As shown in figure 5, the circulating vapor phase creates bubbles in the middle of the cell volume that homogenize the phase's gradients and improve convective heat transfer to the walls. To further increase convective heat transfer between the phases and between the fluid and the wall, a porous cap on top of the entry may be used, that dispenses the bubbles in the whole cell volume.

## 5. Conclusion and outlook

A data set of 9 points of the nitrogen vapor-liquid coexistence curve is measured during the commissioning of CryoPHAEQTS. The  $p$ - $T$  data is in good accordance with the REFPROP database yielding an AAD of 0.8%. The results show an inhomogeneous temperature distribution in the equilibrium cell, yielding a vertical temperature difference of up to 220 mK. By enhanced thermal coupling and shielding, the measurement accuracy of CryoPHAEQTS will be further improved.

Next, the test stand will be equipped with a novel cryogenic mass flow meter [6, 7] in combination with a Coriolis mass flow meter at ambient temperature in order to determine the specific heat capacity of the vapor phase in equilibrium. For transport properties such as viscosity, diffusivity and thermal conductivity, an optical system will be installed for dynamic light scattering measurements.

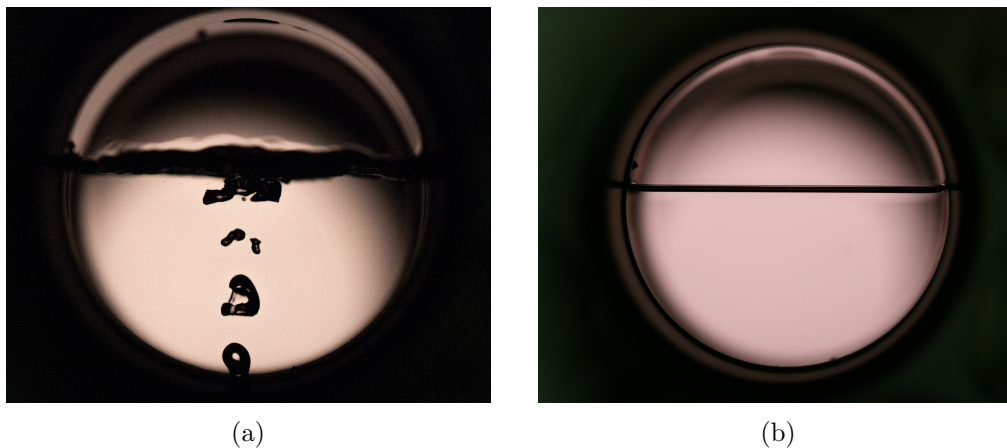


Figure 5: Vapor-liquid coexistence of nitrogen in the equilibrium cell with gas phase circulation (a) and without (b).

## 6. References

- [1] Lemmon Eric W, Huber Marcia L, McLinden Mark O 2018 Refprop: Reference fluid properties
- [2] Tamson J, Stamm M and Grohmann S 2019 *IOP Conference Series: Materials Science and Engineering* **502** 012087
- [3] Peper S, Fonseca J M and Dohrn R 2019 *Fluid Phase Equilibria* **484** 126–224 ISSN 03783812
- [4] Joint Committee for Guides in Metrology Jcgm 100: Evaluation of measurement data - guide to the expression of uncertainty in measurement
- [5] Span R, Lemmon E W, Jacobsen R T, Wagner W and Yokozeki A 2000 *Journal of Physical and Chemical Reference Data* **29** 1361–1433 ISSN 0047-2689
- [6] WEKA AG 2018 <sup>WEKA</sup>Sense<sup>®</sup> URL <https://www.wekasense.ch>
- [7] Grohmann S 2014 *Cryogenics* **60** 9 – 18

## Acknowledgements

The authors would like to acknowledge the support from the Karlsruhe School of Elementary Particle and Astroparticle Physics: Science and Technology (KSETA).